

Electrochemical measurements were done with the help of a PAR Model 370-4 electrochemistry system incorporating a Model 174A polarographic analyzer, a Model 175 universal programmer, a Model RE 0074 X-Y recorder, a Model 173 potentiostat, a Model 179 digital coulometer, and a Model 377A cell system. A platinum wire and a saturated calomel electrode (SCE) were used as auxiliary and reference electrodes, respectively. Solutions were deaerated with purified dinitrogen and experiments were conducted at 298 K under dinitrogen atmosphere. The potentials are uncorrected for junction contribution.

(b) **Procedures.** The basal pyrolytic graphite electrodes were freshly cleaved with a razor blade just prior to use. A freshly prepared solution (0.005–0.5 wt %) of P-SSH in 1:1 water-methanol was used for coating. The coating could be achieved in two ways: (i) dipping of electrode into a solution of the polymer for 15 min; (ii) transferring measured aliquots (5 μ L) of the polymer solution to the surface of the electrode. In either case the solvent was allowed to evaporate slowly at room temperature. In most experiments reported in this work procedure ii was utilized.

For loading, the coated electrodes were immersed in stirred solutions of $(0.02\text{--}1.05) \times 10^{-3}$ M $[\text{NiL}](\text{ClO}_4)_2$ in the buffer of required pH. Cyclic voltammograms were recorded from time to time till a leveling off of the increased peak current occurred (about 10 min). The electrodes were then removed from the loading solution and briefly rinsed with the same buffer solution without any NiL^{2+} . The electrodes were then carefully dried and finally transferred to pure buffer solution for electrochemical studies.

For determining surface coverage, Γ_{Ni} (i.e. the quantity of NiL^{2+} incorporated by P-SS films per unit area of the electrode), the loaded electrodes were placed in pure buffer and coulometry was performed by holding the potential at values well below the voltammetric peak potential

for the reduction of the incorporated NiL^{2+} . Surface coverage was calculated from the relation $\Gamma_{\text{Ni}} = Q/nFA$, where n is the number of electrons transferred per molecule reduced, F is Faraday's constant, A is the area of the electrode in cm^2 , and Q is the total charge consumed for the reduction of the bound NiL^{2+} . All reported coverage data (corrected for background contributions) are averages of at least three independent measurements. The results are reproducible to within $\pm 20\text{--}30\%$.

The effective concentrations (mol/L) of NiL^{2+} in the P-SS films, $[\text{NiL}^{2+}]_p$, were calculated²⁴ from eq 7 where A is the electrode area and

$$[\text{NiL}^{2+}]_p = 10^3 A \Gamma_{\text{Ni}} / \beta_p \quad (7)$$

β_p is the volume of polymer film. The value of β_p is calculated from the mass of P-SS in the film, and the polymer film density is taken as roughly equal to the bulk density (1.33 g/cm^3).

The rate constant for the loss of NiL^{2+} from the loaded electrode was calculated from the slope of the semilogarithmic plot of cathodic peak current vs. the time the electrode was exposed to the buffer solution (298 K). The observed rate constant $(3.05 \pm 0.5) \times 10^{-4} \text{ s}^{-1}$ is the average of four experiments.

Acknowledgment. Financial help received from the Department of Science and Technology, Government of India, New Delhi, India, is gratefully acknowledged. Constructive comments of reviewers were very helpful at the revision stage.

Registry No. $\text{Ni}^{\text{II}}(\text{H}_2\text{L})^{2+}$, 55188-31-3; $\text{Ni}^{\text{II}}(\text{HL})^+$, 60306-03-8; $\text{Ni}^{\text{II}}\text{L}$, 59980-38-0; $\text{Ni}^{\text{III}}\text{L}^+$, 59980-37-9; $\text{Ni}^{\text{IV}}\text{L}^{2+}$, 55188-33-5; P-SS, 28210-41-5; P-SS (sodium salt), 25704-18-1; graphite, 7782-42-5.

Contribution from the Dipartimento di Chimica Analitica, Università di Torino, 10125 Torino, Italy, and Max-Planck-Institut für Biophysikalische Chemie, 3400 Göttingen, West Germany

Electron-Transfer Kinetics of 4,4'-Bis(alkoxycarbonyl)-2,2'-bipyridine-Iron Complexes in Micellar Solution

Marco Vincenti,[†] Edmondo Pramauro,[†] Ezio Pelizzetti,^{*†} Stephan Diekmann,[‡] and Jens Frahm[‡]

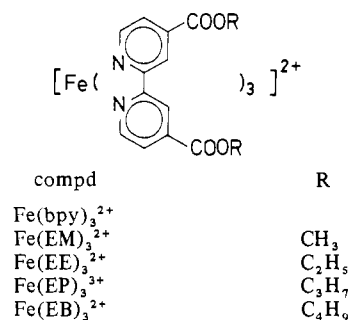
Received January 16, 1985

The kinetics of electron-transfer reactions of a series of iron complexes $\text{Fe}(\text{EX})_3^{2+}$ ($\text{EX} = 4,4'$ -bis(alkoxycarbonyl)-2,2'-bipyridine, with alkoxy = methoxy, ethoxy, propoxy, butoxy) have been studied in homogeneous and in micellar solution. In homogeneous solution the rates of electron-transfer reactions with aquocerium(IV) ions are similar for the different complexes. In the presence of anionic micelles of sodium dodecyl sulfate the observed rate constants are enhanced as compared to those in homogeneous solution. At high surfactant concentrations, the rate enhancement is similar for the different $\text{Fe}(\text{EX})_3^{2+}$ complexes investigated, whereas in the region of the critical micelle concentration relevant differences occur. By the use of a theoretical description of the diffuse double layer previously developed, the electrostatic enrichment of counterions at the micellar surface turns out to be the dominating contribution to the overall rate enhancement. If the overall enhancement is divided by the electrostatic part, additional contributions due to alterations of the second-order rate constant in the micellar environment are found. At low surfactant concentrations the results suggest a formation of "micelles" of altered size and shape, which are able to solubilize more than one iron complex. Among these iron complexes charge delocalization effects might occur and further contribute to the rate enhancement.

Introduction

Electron-transfer reactions in organized structures have been extensively investigated in relation to the solar energy conversion¹ and the redox processes in biological systems.² Although effects of micelles on electron-transfer rates have received attention, they have been analyzed only in terms of conventional kinetic models.³ Recently, an attempt has been made to separate the electrostatic from the nonelectrostatic contribution to the apparent overall rate constant. This approach was successfully applied to reactions between aquoions and organic molecules⁴ as well as metal complexes with organic ligands.⁵ In order to investigate the effect of increasing hydrophobicity on the kinetic properties of metal complexes with organic ligands, the iron complexes $\text{Fe}(\text{EX})_3^{2+}$

Chart I



[†] Università di Torino.

[‡] Max-Planck-Institut für Biophysikalische Chemie.

($\text{EX} = 4,4'$ -bis(alkoxycarbonyl)-2,2'-bipyridine, with alkoxy = methoxy (EM), ethoxy (EE), propoxy (EP), and butoxy (EB))

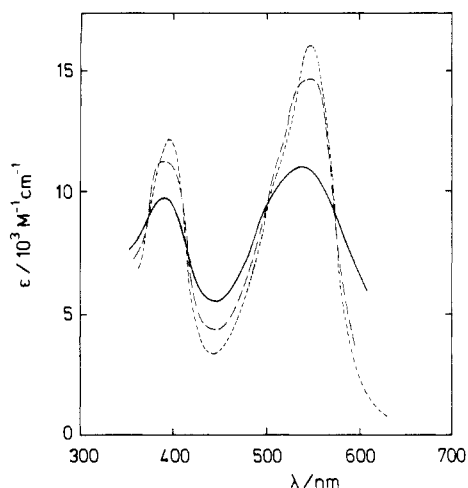


Figure 1. Spectra of $\text{Fe}(\text{EX})_3^{2+}$ complexes: (---) $\text{Fe}(\text{EE})_3^{2+}$ in aqueous solution; (—) $\text{Fe}(\text{EM})_3^{2+}$ in 0.02 M SDS; (- - -) $\text{Fe}(\text{EB})_3^{2+}$ in 0.02 M SDS.

were prepared and characterized (see also Chart I). Their kinetic properties were investigated in the presence of sodium dodecyl sulfate (SDS) as micelle forming surfactant, with Ce(IV) used as oxidant.

Experimental Section

The preparation of the free ligands and the metal complexes, as well as an electrochemical characterization with cyclic voltammetry measurements, are reported elsewhere.⁶ SDS (FLUKA) was purified by recrystallization. UV-visible spectra of the complexes were recorded with a CARY 219 spectrophotometer.

Kinetic Measurements. Kinetic runs were carried out by means of a Durrum stopped-flow spectrophotometer, at 25 °C. The wavelength used was that of the maximum absorption of the $\text{Fe}(\text{EX})_3^{2+}$ complexes (547 nm). Solutions of both reactants were prepared immediately before use (in the case of Ce(IV) this avoids the formation of polymeric species).⁷

For the kinetic runs in homogeneous solution, the initial concentration of $\text{Fe}(\text{EX})_3^{2+}$ was 1×10^{-5} M while the Ce(IV) concentration ranged between 5×10^{-4} and 5×10^{-3} M.

For the kinetic runs in surfactant solutions, the experiments were repeated several times at fixed concentrations: $[\text{Fe}(\text{EX})_3^{2+}] = 3 \times 10^{-6}$ M, and $[\text{Ce}(\text{IV})] = 3 \times 10^{-5}$ M. For some experiments the concentration range of the surfactant was limited by precipitation or turbidity. No experimental evidence was found for a chemical reaction between Ce^{4+} and the dissociated surfactant molecules in the micelle. Since SDS is an ionic surfactant, the ionic strength increases with surfactant concentration. In order to keep the ionic strength constant at low SDS concentrations, 0.05 M HNO_3 was added to all solutions. Problems associated with slow hydrolysis of dodecyl sulfate have been avoided by adding SDS to the solutions immediately before the measurement.

Cmc Measurements. Since the addition of electrolytes or solubilizers to surfactant solutions decreases the cmc (critical micelle concentration),^{8,9} surface tension (γ) measurements have been performed with a Kruss tensiometer. Plots of γ vs. the logarithm of surfactant concentration resulted in graphs consisting of two linear parts. The bulk phase

Table I. Iron Complexes and Their Second-Order Rate Constants with Ce(IV)

compd	$k_{\text{H}_2\text{O}}/\text{M}^{-1} \text{s}^{-1}$	compd	$k_{\text{H}_2\text{O}}/\text{M}^{-1} \text{s}^{-1}$
$(\text{bpy})_3\text{Fe}(\text{ClO}_4)_2$	6.0×10^3	$(\text{EE})_3\text{Fe}(\text{ClO}_4)_2$	3.1×10^2
$(\text{EB})_3\text{Fe}(\text{ClO}_4)_2$	1.3×10^{2b}	$(\text{EM})_3\text{Fe}(\text{ClO}_4)_2$	1.8×10^2
$(\text{EP})_3\text{Fe}(\text{ClO}_4)_2$	2.3×10^2		

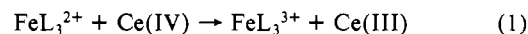
^a All compounds were synthesized except $(\text{bpy})_3\text{Fe}(\text{ClO}_4)_2$ (purchased from FLUKA). ^b Estimated.

concentration at the point of intersection of these two lines was taken as the cmc of the system containing the reaction partners adjusted to the ionic strength and pH. The cmc was measured after the electron-transfer reaction occurred. For example, with initial conditions $[\text{Fe}(\text{EM})_3^{2+}] = 3 \times 10^{-6}$ M, $[\text{Ce}(\text{IV})] = 3 \times 10^{-5}$ M, and ionic strength $\mu = 0.05$ M, a cmc value of ca. 1×10^{-3} M was found. The uncertainty of the cmc values is due to the innate lability of the $\text{Fe}(\text{EX})_3^{2+}$ complexes. For the other complexes an upper limit is $\text{cmc} \leq 5 \times 10^{-4}$ M. Fortunately, this uncertainty does not disturb the quantitative kinetic treatment (see below).

Results and Discussion

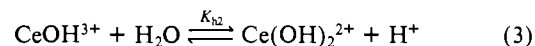
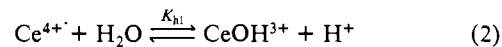
Spectral Properties of the Complexes. The visible spectra in aqueous solution are very similar for all $\text{Fe}(\text{EX})_3^{2+}$ complexes. With respect to the parent $\text{Fe}(\text{bpy})_3^{2+}$ the wavelength of the maximum absorption is shifted from 528 to 547 nm. The molar absorptivity increases slightly from 1.2×10^4 to $1.6 \times 10^4 \text{ M}^{-1} \text{ cm}^{-1}$.¹⁰ Only the spectrum of $\text{Fe}(\text{EE})_3^{2+}$ in aqueous solution is shown in Figure 1. The similarity of the spectra for the different complexes indicates the small influence of the length of the alkyl chain on the electronic structure of the complexes. A slightly different behavior is observed in the presence of SDS micelles. In Figure 1 the spectra of $\text{Fe}(\text{EM})_3^{2+}$ and $\text{Fe}(\text{EB})_3^{2+}$ in the presence of 0.02 M SDS are reported: the bands broaden with increasing alkyl chain, suggesting different interactions of the complexes with the micellar structure.

Kinetics in Homogeneous Solutions. The rate constants of the overall reaction

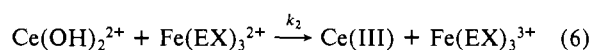
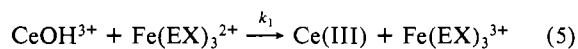
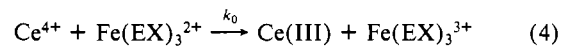


were determined under pseudo-first-order conditions ($[\text{FeL}_3^{2+}] = 1 \times 10^{-5}$ M, $[\text{Ce}(\text{IV})] = 5 \times 10^{-4}$ to 5×10^{-3} M, $[\text{H}^+] = 0.05$ M, and $\mu = 0.05$ M). In addition, the second-order rate constant of $\text{Fe}(\text{bpy})_3^{2+}$ was measured. All values are listed in Table I. The rates of the $\text{Fe}(\text{EX})_3^{2+}$ complexes in aqueous solutions do not vary significantly with the chain length of the alkoxy group (a slight maximum is observed for $\text{Fe}(\text{EE})_3^{2+}$). Thus, in homogeneous solution the Ce^{4+} ions seem to approach the $\text{Fe}(\text{EX})_3^{2+}$ complexes without additional hindrance due to the increased chain lengths. Measurements were also performed at different acidities and ionic strengths.⁶

The aquocerium(IV) ion in solution exists in different hydrolyzed species:¹¹



From the data reported for K_{h1} and K_{h2} it is conceivable that at least three different paths can participate in the reaction process:



hence

$$k_{\text{exptl}} = \frac{(k_0[\text{H}^+]/K_{h1}) + k_1 + (k_2K_{h2}/[\text{H}^+])}{([\text{H}^+]/K_{h1}) + 1 + (K_{h2}/[\text{H}^+])} \quad (7)$$

- Henglein, A.; Grätzel, M. In "Solar Power and Fuels"; Bolton, J. R., Ed.; Academic Press: New York, 1977. Calvin, M. *Acc. Chem. Res.* **1978**, *11*, 369-379. Pelizzetti, E. In "Physics of Amphiphiles. Micelles, Vesicles and Microemulsions"; Degiorgio, V., Corti, M., Eds.; North Holland: Amsterdam, 1985; pp 513-523.
- Fendler, J. H. "Membrane Mimetic Chemistry"; Academic Press: New York, 1982.
- Bhalekar, A. A.; Engberts, J. B. *J. Am. Chem. Soc.* **1978**, *100*, 5914-5920. Bunton, C. A.; Cerichelli, G. *Int. J. Chem. Kinet.* **1980**, *12*, 519-533. Pelizzetti, E.; Pramauro, E. *Inorg. Chem.* **1980**, *19*, 1407-1409.
- Minero, C.; Pramauro, E.; Pelizzetti, E.; Meisel, D. *J. Phys. Chem.* **1983**, *87*, 399-407.
- Pramauro, E.; Pelizzetti, E.; Diekmann, S.; Frahm, J. *Inorg. Chem.* **1982**, *21*, 2432-2436.
- Vincenti, M.; Pramauro, E.; Pelizzetti, E.; Geiger, T. *Atti Accad. Sci. Torino, Cl. Sci. Fis., Mat. Nat.*, in press.
- Samuni, A.; Czapski, G. *J. Chem. Soc., Dalton Trans.* **1973**, 487-488.
- Kratohvil, S.; Shinoda, K.; Matijevic, E. *J. Colloid Interface Sci.* **1979**, *72*, 106-112.
- Rosen, M. J. "Surfactants and Interfacial Phenomena"; Wiley: New York, 1978.

(10) Ford-Smith, M. H.; Sutin, N. *J. Am. Chem. Soc.* **1961**, *83*, 1830-1834.

(11) Burgess, J. "Metal Ions in Solution", Ellis Horwood: Chichester, England, 1978.

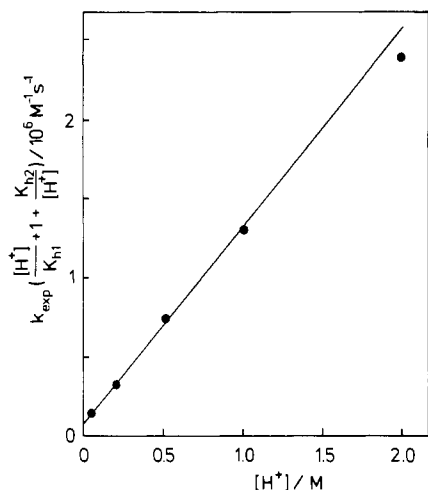


Figure 2. Plot according to eq 7 for the reaction of Ce(IV) with Fe(EE)₃²⁺ in aqueous solution at 25 °C, $\mu = 2.0$ M.

Table II

[SDS], 10 ³ M	rate constant, ^a mol ⁻¹ s ⁻¹			
	Fe(EM) ₃ ²⁺	Fe(EE) ₃ ²⁺	Fe(EP) ₃ ²⁺	Fe(EB) ₃ ²⁺
0.3		2.0 × 10 ⁴	3.3 × 10 ⁵	
0.4		7.5 × 10 ⁴	7.8 × 10 ⁵	
0.5		1.9 × 10 ⁵	1.2 × 10 ⁶	
0.6		3.3 × 10 ⁵	1.6 × 10 ⁶	
0.8		6.4 × 10 ⁵	2.3 × 10 ⁶	
1.0		5.8 × 10 ⁵	2.5 × 10 ⁶	
1.2	1.5 × 10 ⁵	1.6 × 10 ⁵	1.3 × 10 ⁶	
1.4	1.9 × 10 ⁵			
1.5	2.1 × 10 ⁵	1.3 × 10 ⁵	6.5 × 10 ⁵	
1.6	1.9 × 10 ⁵			
1.7	1.7 × 10 ⁵	9.7 × 10 ⁴	3.2 × 10 ⁵	6.1 × 10 ⁵
2.0	1.2 × 10 ⁵	9.3 × 10 ⁴	9.1 × 10 ⁴	4.2 × 10 ⁵
2.2				1.5 × 10 ⁵
2.5	7.1 × 10 ⁴	8.0 × 10 ⁴	8.3 × 10 ⁴	9.6 × 10 ⁴
3.0	5.8 × 10 ⁴	6.5 × 10 ⁴	5.8 × 10 ⁴	6.5 × 10 ⁴
3.5	4.7 × 10 ⁴	4.4 × 10 ⁴	5.0 × 10 ⁴	5.1 × 10 ⁴
4.0	3.9 × 10 ⁴	3.8 × 10 ⁴	4.3 × 10 ⁴	4.3 × 10 ⁴
5.0	2.8 × 10 ⁴	3.0 × 10 ⁴	3.1 × 10 ⁴	3.0 × 10 ⁴
8.0		1.6 × 10 ⁴		

^a At 25 °C and 50 mM HNO₃.

Figure 2 shows a plot of $k_{\text{exp}} \left(\frac{[\text{H}^+]}{K_{\text{h1}}} + 1 + \frac{K_{\text{h2}}}{[\text{H}^+]} \right)$ as a function of $[\text{H}^+]$ for Fe(EE)₃²⁺ using values for K_{h1} , 6.2 mol⁻¹, and K_{h2} 0.14 mol⁻¹ taken from the literature.^{12,13} The linearity suggests that the contribution of path 6, involving Ce(OH)₂²⁺, is negligible. Since the estimated value for k_0 , 9×10^6 M⁻¹ s⁻¹, is much larger than k_1 , found to be 1×10^5 M⁻¹ s⁻¹, the predominant reactive species is assumed to be Ce⁴⁺. Thus, contributions from CeOH³⁺ and Ce(OH)₂²⁺ were neglected for the kinetic treatment. This is in agreement with the finding that for outer-sphere electron transfer the less hydrolyzed species are the most reactive.^{14,15} In perchlorate or nitrate media, however, previous investigations have shown that the hydrolyzed species is more reactive.^{16,17}

Kinetics in Micellar Solutions. The kinetic data measured in the presence of SDS are presented in Table II. When micellar aggregates are present, the iron complexes are solubilized in the

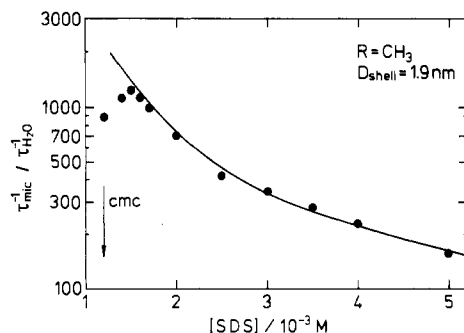


Figure 3. Experimental rates in micellar solution τ_{mic}^{-1} relative to rates in water $\tau_{\text{H}_2\text{O}}^{-1}$ as a function of the surfactant concentration for the reaction of Fe(EM)₃²⁺ with Ce(IV) (●). In addition the theoretical electrostatic enhancement factor f_{e1} is plotted for the surface shell thickness $D_{\text{shell}} = 1.9$ nm (—). The cmc (1.2×10^{-3} M) of the system is indicated.

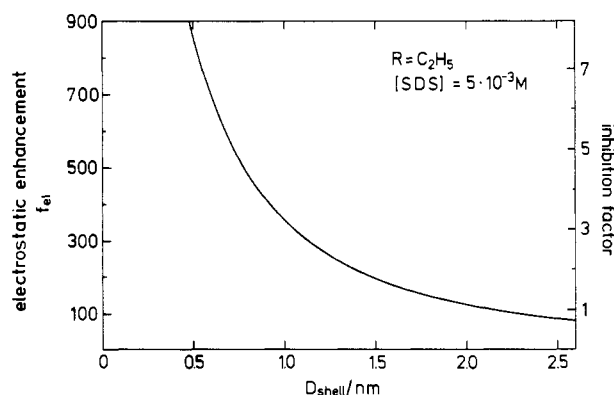


Figure 4. Electrostatic enhancement factor f_{e1} (left scale) and inhibition factor (right scale) plotted vs. D_{shell} for the system Fe(EE)₃²⁺ at $[\text{SDS}] = 5 \times 10^{-3}$ M.

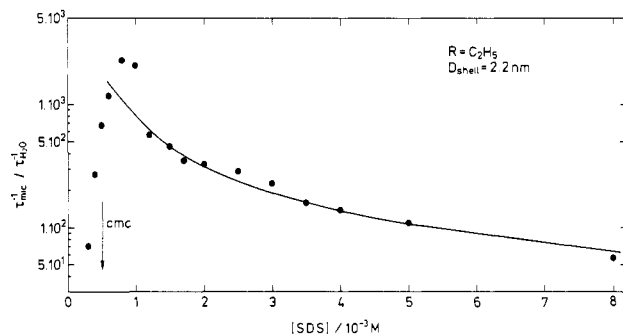


Figure 5. Experimental rates in micellar solution τ_{mic}^{-1} relative to rates in water $\tau_{\text{H}_2\text{O}}^{-1}$ as a function of the surfactant concentration for the reaction of Fe(EE)₃²⁺ with Ce⁴⁺. The cmc of this system is 0.5×10^{-3} M.

micelles, whereas the highly positively charged Ce⁴⁺ counterions are distributed in the diffuse double layer. In a discussion of the micellar effect on the overall reaction rate, only the value relative to the reaction rate in aqueous solution is of interest (compare Table I). Correspondingly, the apparent reaction rate measured in the micellar system is divided by the rate in the absence of micelles. In the following discussion only the relative rate enhancement is considered. These data are displayed in Figures 3 and 5 for the systems Fe(EM)₃²⁺ and Fe(EE)₃²⁺, respectively, and, divided by the electrostatic contribution to the overall rate enhancement, in Figure 6. Alterations of the rates in micellar solution are expected due to electrostatic enrichment or dilution of counterions at the micellar surface and environmental influences on the intrinsic rate constant.

Electrostatic Model and Calculation. The model of a micellar solution adopted here assumes the micelles to be spheres with a homogeneous surface charge. In a preceding paper,¹⁸ the micellar

- (12) Everett, K. G.; Skoog, D. A. *Anal. Chem.* **1971**, *43*, 1541–1547.
- (13) Hanna, S. B.; Kessler, R. R.; Merbach, A.; Ruzicka, S. *J. Chem. Educ.* **1976**, *53*, 524–527.
- (14) McAuley, A. *Coord. Chem. Rev.* **1970**, *5*, 245–273.
- (15) Pelizzetti, E.; Giordano, R. *J. Chem. Soc., Dalton Trans.* **1979**, 1516–1518. Pelizzetti, E. *J. Chem. Soc., Dalton Trans.* **1980**, 484–486.
- (16) Adamson, M. G.; Dainton, F. S.; Glentworth, P. *Trans. Faraday Soc.* **1965**, *61*, 689–701.
- (17) Candlin, J. P.; Taylor, K. A.; Thompson, D. T. "Reactions of Transition Metal Complexes"; Elsevier: Amsterdam, 1968.

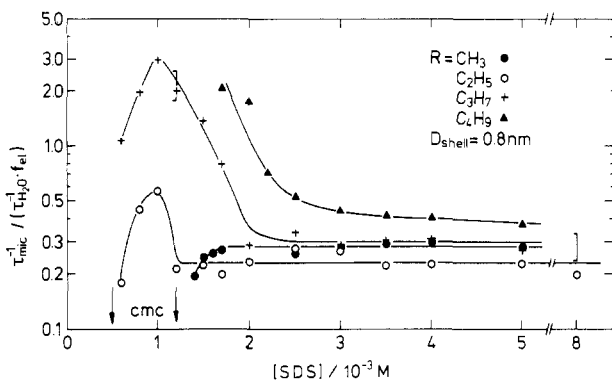


Figure 6. Observed rates in micellar solution relative to rates in water divided by the electrostatic enhancement factor f_{e1} (for $D_{shell} = 0.8$ nm) for the four analyzed systems vs. SDS concentration. The cmc's for the different systems are indicated (the three systems with the long chain lengths are assumed to have the same cmc). At $[SDS] = 1.2 \times 10^{-3}$ M the influence of the different micellar parameters (aggregation number, surface potential, and radius) was tested. The variation in f_{e1} is included as an "error" bar to the data point of the $Fe(EP)_3^{2+}$ system. Obviously the variation in f_{e1} due to the experimental uncertainty of the used micellar parameters is not able to explain the strong rate enhancement in the close vicinity of the cmc. The error of the horizontal lines (their ordinate values give the inhibition factors) is determined by the experimental error in k_{H_2O} . Its value, identical for all four systems, is indicated by an error bar at $[SDS] = 8 \times 10^{-3}$ M.

surface potentials of sodium alkyl sulfates have been measured by using two fluorescent pH indicators under a variety of conditions (salt, chain length, temperature). The micellar radius, r_{mic} , and the aggregation number, m , are taken from the literature.¹⁹ In the presence of salt, the radius r_{mic} has been correlated to the third root of the mean aggregation number. For the experimental conditions analyzed in this paper, the micellar parameters m , r_{mic} , and the surface potential are interpolated from the known values (for the cmc see the Experimental Section). The numerical procedure is based on a modified nonlinearized Poisson-Boltzmann equation, which computes the local ion concentrations in the diffuse double layer around a micelle as a function of distance from the micellar surface. It allows for the effects of finite ion sizes and the dependence of the dielectric constant on the local electrical field strength.²⁰ The radii of the hydrated ions as well as co-ions are taken to be 0.25 nm. This value corresponds to the radius of the hydrated sodium ion (the counterion of the surfactant molecule) and has been taken as an average value for the monovalent ions present.

In order to describe electron-transfer reactions between ligands solubilized in micelles and counterions distributed in the diffuse double layer, "surface" concentrations of these ions have to be computed by taking into account that such reactions proceed within specific reaction distances. In more detail, the electrostatic attraction of the Ce^{4+} ions to the micellar surface leads to a local increase of their concentration. This effect can be described by a factor f_{e1} , which is calculated by the electrostatic theory.²⁰ The iron complexes solubilized in the micelles are assumed to react only with those Ce^{4+} ions that are in close vicinity to the micellar surface, i.e. within a distance D_{shell} from the surface plane. Thus, the actual reaction volume can be treated as a spherical shell of thickness D_{shell} around the micelle, yielding the "surface" concentration. Since the micellar radius is known¹⁸ and assumed to be unchanged by solubilization of a complex, the reaction volume is only dependent on D_{shell} . The number of counterions in this shell is determined by integrating the appropriate ion distribution (Ce^{4+}) from the micellar radius to D_{shell} . If this number is divided by the number of corresponding ions in the same volume of the aqueous solution without micelles (mean weighed-in concentra-

tion), the factor f_{e1} is obtained. For example, for a surfactant concentration of 3 mM, a cmc of 1.2 mM, an aggregation number of 80, a micellar radius of 2.04 nm, and a surface potential of -90 mV one calculates about 2 Ce^{4+} ions and 15 monovalent ions to be located within a shell of 0.8-nm thickness. The corresponding weighed-in concentrations are 5×10^{-5} M for Ce^{4+} and 0.052 M monovalent ions, leading to electrostatic enhancement factors f_{e1} of 1185 and 8, respectively.

At high surfactant concentrations, simpler electrostatic models might be applied that, for example, assume all counterions to be bound to the micellar surface.²¹ Such models, however, fail at surfactant concentrations close to the cmc where the number of micelles becomes small.²² Thus, at least effects of volume saturation of the counterions as well as of an altered dielectric constant at the micellar surface have to be taken into account. On the other hand, even more detailed models of the micellar surface might easily be considered. For example, the actual distances of the counterions in the double layer from the micellar surface might be used directly to calculate probabilities for electron-transfer reactions of all Ce^{4+} ions in solution. Such detailed models, however, introduce a variety of new parameters and, therefore, do not allow a check of the consistency of the theory. In contrast, the present model of the micellar solution has been successfully applied to the quantitative description of the rate enhancement of reactions at the micellar surface^{5,22} as well as rate inhibition in the bulk in between the micelles.²³ Here, it is applied with only a single variable parameter, the surface shell thickness D_{shell} , which is determined by the electron-transfer reaction. This parameter has a clear physicochemical meaning and can be chosen only within a narrow range of values.

Rate Enhancement at High Surfactant Concentrations. The dependence of the electrostatic factor f_{e1} for Ce^{4+} upon surfactant concentration is given in Figure 3. Considering only electrostatic enrichment, the data for the reaction between $Fe(EM)_3^{2+}$ and Ce^{4+} can be quantitatively explained by assuming a surface shell of thickness $D_{shell} = 1.9$ nm defining the reaction volume. However, D_{shell} should not be fitted to the experimental data but adjusted to the largest distance between reaction partners still reacting. In general, for electron-transfer reactions the tunneling distance is assumed to be the shortest possible geometrical distance, i.e. about the sum of the molecular radii of the reacting species.²⁴ This is because the tunneling probability decreases strongly with increasing distance and leads to a value that generally does not exceed 1 nm.²⁵ Also for the present reactions, geometrical considerations suggest a reasonable distance of about 0.5–1.0 nm (the radius of the hydrated Ce^{4+} ion is 0.4 nm;²⁶ the diameter of a pyridine ring is 0.5 to 0.6 nm). When $D_{shell} = 0.8$ nm is chosen instead of $D_{shell} = 1.9$ nm, the electrostatic factor f_{e1} increases by a factor of 3 due to a higher local ion concentration in the vicinity of the micellar surface: the absolute number of Ce^{4+} counterions in the smaller reaction volume decreases, but the relative concentration, i.e. the number of ions per volume, increases with respect to the concentration in the homogeneous phase. However, the general shape of the curve (f_{e1} as a function of surfactant concentration) does not change, so that the curve in Figure 3 is shifted upward to higher rates for smaller values of D_{shell} . If the experimental rates are divided by f_{e1} for $D_{shell} = 0.8$ nm, a value of about 0.3 is obtained, which is independent of the surfactant concentration (see Figure 6). Thus, if realistic reaction distances are introduced, an inhibition factor of about 3 is found. The complementary variation of the electrostatic enhancement factor f_{e1} and the inhibition factor is displayed in Figure 4 for the system

(18) Frahm, J.; Diekmann, S.; Haase, A. *Ber. Bunsenges. Phys. Chem.* **1980**, *84*, 566–571.

(19) See literature quoted in ref 18.

(20) Frahm, J.; Diekmann, S. *J. Colloid Interface Sci.* **1979**, *70*, 440–447.

(21) James, A. D.; Robinson, B. H. *J. Chem. Soc., Faraday Trans. 1* **1978**, *74*, 10–21.

(22) Diekmann, S.; Frahm, J. *J. Chem. Soc., Faraday Trans. 1* **1979**, *75*, 2199–2210.

(23) Diekmann, S.; Frahm, J. *J. Chem. Soc., Faraday Trans. 1* **1980**, *76*, 446–447.

(24) Marcus, R. A. *J. Chem. Phys.* **1965**, *43*, 679–701.

(25) Gordon, B. M.; Williams, L. L.; Sutin, N. *J. Am. Chem. Soc.* **1961**, *83*, 2061–2064.

(26) Sutin, N. *Annu. Rev. Nucl. Sci.* **1962**, *12*, 285–328.

Fe(EE)₃²⁺ at a surfactant concentration of 5×10^{-3} M.

Rate inhibition might be understood as the influence of the micellar environment on the reaction, causing a change of the true second-order rate constant for the reaction taking place at the micellar surface. The high surface potential of the micelle and the low dielectric constant particularly influence the electronic system of the iron complex solubilized within the micelle. Inhibition and acceleration of electron-transfer reactions at micellar surfaces have been found for other systems as well, e.g. an inhibition factor of about 5 was observed for the system Os(dmbpy)₃²⁺/Fe³⁺/SDS.⁵

The reaction between Fe(EE)₃²⁺ and Ce⁴⁺ can be understood on a similar basis. Again, nearly the entire range of surfactant concentrations could be explained by f_{e1} using the surface shell thickness to be 2.2 nm (see Figure 5). However, this value is too large for an electron-transfer reaction. Assuming $D_{\text{shell}} = 0.8$ nm, an inhibition factor of about 3 has to be taken into account (deviations close to the cmc will be discussed below). Also for the electron-transfer reactions of Fe(EP)₃²⁺ and Fe(EB)₃²⁺ with Ce⁴⁺ inhibition factors are found for realistic reaction distances (see Figure 6). The inhibition factors of the four different systems vary slightly. Although the variation is within experimental error (see Figure 6), the inhibition factor decreases in the order Fe(EE)₃²⁺ > Fe(EP)₃²⁺ > Fe(EB)₃²⁺. This trend parallels the decrease in the relative rates found for these systems comparing aqueous solutions to aqueous organic solvent mixtures.⁶

It should be noted that the theoretical model used here does not include detailed assumptions on the molecular arrangement at the micellar surface. Although rate enhancements of several reactions are quantitatively described, no absolute values for reaction distances can be obtained. For the present systems the assumed reaction distances are based on molecular considerations. The inhibition factors are determined by the reaction distance. However, they are independent of the electrostatic theory itself as well as of the rate contribution discussed below. Different reaction distances and consequently different inhibition factors (see Figure 4) only shift the scale of the vertical axis in Figure 6. In addition we note that for a similar system⁵ inhibition and acceleration factors were determined for forward and reverse reactions, respectively.

Rate Enhancement at Low Surfactant Concentrations. At surfactant concentrations well above the cmc, the micelle concentration is so large that only one iron complex is solubilized per micelle, whereas most micelles do not contain a reactant at all. Only under these experimental conditions can micelles be assumed to be unchanged in size and shape. For the present systems involving the long-chain EE, EP, and EB complexes, we have experimental evidence that this is not fulfilled in concentration ranges close to the cmc. In these systems, the measured rates increase well beyond the value predicted by electrostatic considerations to yield a maximum at about 0.001 M surfactant concentration (see Figure 6). It turns out that the longer the chain lengths (C₃H₇ and C₄H₉) the more pronounced is the maximum. Increasing the surfactant concentration decreases the experimental rate sharply to the value found after correction for the electrostatic and environmental influences (as outlined in the previous sections).

The rate maximum close to the cmc is observed at surfactant concentrations at which more than one iron complex may be assumed to be bound to some micelles.²⁷ Explanations of the rate maximum on the basis of normal micelles are not successful. For example, if normal micelles are assumed, then the micelle concentration would already equal the concentration of the iron complex (3×10^{-6} M) at a surfactant concentration of 7.5×10^{-4} M. Thus, the rate is maximum at a SDS concentration at which the number of micelles exceeds the number of complexes. Consequently, no additional rate enhancement should be observed. Close to the cmc, also the assumption of a large number of *small*

micelles with only one complex bound per "micelle" fails in a similar way: the electrostatic enhancement factor would even be decreased due to the dilution of the counterions at the surfaces of the large number of micelles.

Consequently, the observed rate maxima seem to be due to aggregates of altered size and composition. This is further supported by the general finding that the complexes bearing ligands with chain length R = C₂H₅, C₃H₇, and C₄H₉ strongly decrease the cmc. This indicates a preferential tendency for self-aggregation or cluster formation, which may lead to mixed aggregates of reactants and surfactants. Moreover, small changes in the absorption spectra of the dyes have been observed in solutions of low surfactant concentration. The suggestion of mixed aggregates is also based on the finding that the surfactant concentration at which the maximum has decreased to the unspecific electrostatic enhancement is different for the different systems (compare Figure 6): a more pronounced aggregation behavior is more probable for ligands with increasing chain length. Correspondingly, higher micelle concentrations are needed for a dissolution of appropriate mixed aggregates and a redistribution of reactants.

Assuming the existence of mixed aggregates at low surfactant concentrations, the rate maximum might be explained as follows. In aggregates with two or more iron complexes, some ligands might have preferred reaction sites that allow the reaction to proceed faster than at other places. If electrons can be exchanged between all iron complexes within a certain aggregate, the reaction may always take place at the preferred sites, obviously increasing the observed electron-transfer rate. In fact, such charge delocalization effects are known for electronic processes in organic crystals²⁸ and for the mobility of charge carriers in organic glasses²⁹ and were experimentally found for electron-transfer reactions involving oxidation and reduction of a photoexcited cyanine dye in monolayer assemblies.³⁰

Conclusions

Electron-transfer reactions between iron complexes with ligands of increasing hydrophobicity and Ce⁴⁺ have been investigated in the absence and presence of micelles. Similar rate constants were obtained in aqueous solution for all complexes. In the presence of anionic micelles, a detailed analysis could be applied, which allowed the separation of electrostatic factors from environmental factors influencing the observed reaction rate. The electrostatic enhancement (and inhibition) is theoretically well understood^{18,20} and has been experimentally confirmed.^{5,22,23} Its contribution to the overall enhancement is predominant. Moreover, a change of the true second-order rate constant for electron-transfer reactions is suggested in cases where ion complexes are involved.⁵ Acceleration⁵ as well as inhibition (ref 5 and this paper) of the reaction has been found and ascribed to environmental influences. Finally, in this paper an additional rate enhancement due to charge delocalization among several complexes solubilized in one "micelle" (or mixed aggregate) has been suggested for the electron-transfer reactions of ions complexed by ligands substituted with long aliphatic side chains.

Acknowledgment. Financial support from NATO (Grant RG 243.82) is gratefully acknowledged. This work was partially supported by the Progetto Finalizzato Chimica Fine e Secondaria, CNR (Rome). Part of this work was performed as the thesis of M.V. at the University of Torino. Helpful discussions with Drs. M. Teubner and D. Möbius are gratefully acknowledged.

Registry No. Fe(EM)₃²⁺, 99148-29-5; Fe(EE)₃²⁺, 83605-82-7; Fe(EP)₃²⁺, 99148-30-8; Fe(EB)₃²⁺, 99148-31-9; Fe(bpy)₃²⁺, 15025-74-8; Ce, 7440-45-1; sodium dodecyl sulfate, 151-21-3.

(27) Berezin, I. V.; Martinek, K.; Yatsimirskii, A. K. *Russ. Chem. Rev. (Engl. Transl.)* **1973**, *42*, 787-802.

(28) Pope, M.; Swenberg, C. E. "Electronic Processes in Organic Crystals"; Clarendon Press: Oxford, England, 1982.
 (29) Bässler, H.; Schönherr, G.; Abkowitz, M.; Pai, D. M. *Phys. Rev. B: Condens. Matter* **1982**, *26*, 3105-3113.
 (30) Möbius, D. *Mol. Cryst. Liq. Cryst.* **1983**, *96*, 319-334. Penner, T. L.; Möbius, D. *J. Am. Chem. Soc.* **1982**, *104*, 7407-7413.